View metadata, citation and similar papers at core.ac.uk
brought to you by CORE
provided by idUS. Depósito de Investigación Universidad de Sevilla

Copyright © 2007 Tech Science Press CMES, vol.17, no.3, pp.215-229, 2007

Hypersingular BEM for Piezoelectric Solids: Formulation and Applications for Fracture Mechanics

J.A. Sanz, M. Solis and J. Dominguez[1]

Abstract: A general mixed boundary element formulation for three-dimensional piezoelectric fracture mechanics problems is presented in this paper. The numerical procedure is based on the extended displacement and traction integral equations for external and crack boundaries, respectively. Integrals with strongly singular and hypersingular kernels appearing in the formulation are analytically transformed into weakly singular and regular integrals. Quadratic boundary elements and quarter-point boundary elements are implemented in a direct way in a computer code. Electric and stress intensity factors are directly computed from nodal values at quarter-point elements. Crack problems in 3D piezoelectric bounded and unbounded solids are solved. The obtained results are shown to be accurate by comparison with other results existing in the literature. The approach presented for the first time in this paper should be useful for future research and development since it can be used in a simple way for general 3D piezoelectric fracture mechanics problems.

Keyword: Boundary element method, Piezoelectric solids, Three-dimensional fracture mechanics.

1 Introduction

Piezoelectric ceramics have been produced since the mid of the 20th century. These materials are the basic ingredient for construction of sensors, transducers, actuators as well as adaptative structures. Lead zirconate titanate (PZT) is the most widely used piezoceramic. There are also piezopolymers as polyvinilidene fluoride (PVDF). Numerical modelling of piezoelectric solids rise certain difficulties since they exhibit not only electro-elastic coupling but anisotropic behaviour. Piezoelectric effect can only appear in crystals that lack of a centre of symmetry; therefore, they are always anisotropic. This anisotropy reduces in most cases to transversal isotropy.

Piezoelectric materials are brittle, and due to manufacturing and complex electromechanical loads, they are likely to develop cracks. The understanding and evaluation of the fracture process in piezoelectric materials are crucial to the advancement of modern intelligent materials.

Among the most significant publications on the field of piezoelectric materials fracture mechanics, one can cite the works of [Barnett and Lothe (1975)], [Parton (1976)], [Deeg (1980)], [Pak (1990)], [Pak (1992)], [Suo, Kuo, Barnett, and Willis (1992)], [Sosa (1992)], [Chen, Shioya, and Ding (2000)] and [Lin, Narita, and Shindo (2003)]. These papers refer to analytical or semi-analytical approaches that introduce same simplifications or can only be applied to some simple geometries. [Kuna (1998)] and [Shang, Kuna, and Abendroth (2003)] have presented a finite element approach for 3D crack problems in piezoelectric materials.

It is well known that the Boundary Element Method (BEM) is a well suited tool for the general analysis of fracture mechanics problems. This fact has led to the publication of different BE approaches for the analysis of cracks in piezoelectric solids in the last few years. Once the BE formulation and implementation for linear elastic fracture mechanics is well

[1] Escuela Superior de Ingenieros, University of Sevilla, 41092 Sevilla, Spain. Corresponding author e-mail address: jose@us.es (J. Dominguez)

established, the main difficulties in the field of piezoelectrics are related to the derivation and integration of fundamental solutions for two and three-dimensional static and dynamic problems. [Pan (1999)] and [Garcia-Sanchez, Saez, and Dominguez (2005)] have presented a single domain formulations for 2D static crack problems in piezoelectrics. Several papers can be cited for wave scattering and time domain piezoelectricity as [Gross, Rangelov, and Dineva (2005)], [Saez, Garcia-Sanchez, and Dominguez (2006)] for crack problems using BEM and [Sladek, Sladek, Zhang, Garcia-Sanchez, and Wunsche (2006)] using the meshless local Petrov-Galerkin Method. A review of the work for 2D problems can be found in these papers.

Few papers and BE formulations for three-dimensional piezoelectric cracked solids have been published. They usually deal with fundamental solutions that require rather complicated numerical evaluation and are restricted to certain types of materials and/or to infinite domain geometries. Some of the most important publications in this field are those presented by [Chen and Lin (1995)], [Zhao, Shen, Liu, and Liu (1997a)], [Zhao, Shen, Liu, and Liu (1997b)], [Ding and Liang (1999)], [Chen (2003a)], [Chen (2003b)], [Ding, Chen, , and Jiang (2004)] and [Chen (2005)]. [Sanz, Ariza, and Dominguez (2005)] have presented a general three-dimensional BE approach for crack problems in piezoelectric materials. It is based on Deeg's fundamental solution [Deeg (1980)] and the classical displacement BIE formulation. A subdomain technique together with quarter-point and singular quarter-point elements are used to evaluated crack extended displacements and extended stress intensity factors (ESIF) for different finite cracked body geometries. Deeg's fundamental solution is general but is not written in an explicit form. It requires of numerical evaluation of an integral for each integration point. A good alternative to Deeg's fundamental solution is that obtained by [Dunn and Wienecke (1996)]. It is limited to transversely isotropic solids but has the great advantage, as compared to other solutions, that is written in a rather compact close form explicit expression that can be easily evaluated. The limitation to transversely isotropic solids is not very restrictive since most piezoelectric ceramics present a transversely isotropic behaviour.

In the present paper, a general mixed BE formulation based on extended displacements and extended traction integral equation for three-dimensional cracked piezoelectric solids is presented for the first time. The traction (and normal electric displacement) integral representation is written for the crack surface and the displacement (and electric potential) integral representation for the external boundaries. The explicit fundamental solution presented by [Dunn and Wienecke (1996)] is used. To do so, it must be differentiated to obtain the corresponding terms for the tractions integral equation representation. The resulting hypersingular and strongly singular terms are regularized by substracting two and one terms of Taylor's series expansion of the extended displacements and tractions at collocation point, respectively. Then, hypersingular and strongly singular expressions around the collocation point, are conveniently transformed in order to apply Stokes' theorem to yield non-singular or weakly singular integrals, which can be numerically evaluated and simple integrals with known analytical solution. Other techniques for dealing with hypersingular kernels integration can be seen in [Sellountos, Vavourakis, and Polyzos (2005)].

Quadratic elements are used for the BE representation of extended displacements and tractions. The elements next to the crack front are quarter-point elements in order to represent properly the crack opening displacement and the electric potential discontinuity near the crack front. Electric and stress intensity factors (ESIF) are computed in a direct way from the opening displacement and electric potential discontinuity at quarter-point nodes. The approach has been implemented in a computer code and numerical examples regarding full space and bounded domain crack problems under mechanical and electrical loading conditions have been analyzed. The obtained results are compared with those existing in the literature.

The approach is completely general and can be used in a simple way for 3D fracture problems with different geometries and loading conditions in piezoelectric solids. It only requires of a simple discretization of the crack surface and external boundaries to yield accurate results. It is the piezoelectric counterpart of the BEM developed for potential problems, isotropic and anisotropic elastic problems by [Dominguez, Ariza, and Gallego (2000)] and [Ariza and Dominguez (2004)].

2 Problem statement

Basic linear equilibrium piezoelectricity equations under static loading, are written in terms of conservation of momemtum and electric charge. In absence of body forces and electric charge, and using the condensed notation introduced by [Barnett and Lothe (1975)], they can be expressed as,

$$\Sigma_{iJ,i} = 0 \tag{1}$$

where lower case indices take values from 1 to 3, while upper case take values 1 to 4. Σ_{iJ} is the stress-electric displacement matrix, defined as,

$$\Sigma_{iJ} = \begin{cases} \sigma_{ij} & \text{for } J = 1,2,3 \\ D_i & \text{for } J = 4 \end{cases} \tag{2}$$

Elastic displacement-electric potential vector U_K is defined as,

$$U_K = \begin{cases} u_k & \text{for } K = 1,2,3 \\ \Phi & \text{for } K = 4 \end{cases} \tag{3}$$

The elastic strain-electric field matrix Z_{Kl} is found through compatibility relationships, and it takes the form,

$$Z_{Kl} = \begin{cases} \frac{1}{2}(u_{k,l} + u_{l,k}) & \text{for } K = 1,2,3, K = l \\ \Phi, l & \text{for } K = 4 \end{cases} \tag{4}$$

The linear constitutive relation in a piezoelectric material is given in terms of elastic, piezoelectric and dielectric constants as follows,

$$\Sigma_{iJ} = E_{iJKl} Z_{Kl} \tag{5}$$

E_{iJKl} being the electroelastic constant matrix,

$$E_{iJKl} = \begin{cases} C_{ijkl} & \text{for } J,K = 1,2,3 \\ e_{lij} & \text{for } J = 1,2,3 \;\; K = 4 \\ e_{ikl} & \text{for } J = 4 \;\; K = 1,2,3 \\ -\varepsilon_{il} & \text{for } J,K = 4 \end{cases} \tag{6}$$

This electroelastic constant matrix, posses major but not minor symmetries being $E_{iJKl} = E_{lKJi}$. It is worthy to remark that due to the piezoelectric microstructure, most piezoelectric materials exhibit an elastically transversely isotropic behaviour with a total number of independent constants equal to 10 (5 elastic, 3 piezoelectric and 2 dielectric).

By virtue of the major symmetry of matrix E_{iJKl}, one can express the stress-electric displacement matrix in terms of the elastic-displacement by inserting Eq. 4 into Eq. 5,

$$\Sigma_{iJ} = E_{iJKl} U_{K,l} \tag{7}$$

Straighforward from Eq. 7, the elastic-traction-normal charge flux vector T_J can be written as,

$$T_J = \Sigma_{iJ} n_i = E_{iJKl} U_{K,l} n_i \tag{8}$$

n_i being the outward normal.

The piezoelectric boundary value problem is considered to be well-posed, once mechanical and electrical boundary conditions are defined. Dirichlet boundary conditions of the problem are,

$$u_i = \overline{u}_i \;\text{ on }\; \Gamma^u \tag{9}$$

$$\Phi = \overline{\Phi} \;\text{ on }\; \Gamma^\Phi \tag{10}$$

where $\overline{u}_i$ and $\overline{\Phi}$ are the prescribed displacements and electric potentials on boundaries Γ^u and Γ^Φ

respectively. Neumann boundary conditions, are written as,

$$\sigma_{ij} \cdot n_j = t_i = \overline{t}_i \text{ on } \Gamma^t \tag{11}$$

$$D_i \cdot n_i = q = \overline{q} \text{ on } \Gamma^q \tag{12}$$

where $\overline{t}_i$ and $\overline{q}$ are the prescribed tractions and normal electric charge flux on the boundaries Γ^t and Γ^q respectively. Obviously, for a well-posed problem, boundaries Γ^u and Γ^t must be disjoint, such that, $\Gamma^u \cap \Gamma^t =$ and the same for the electric part $\Gamma^\Phi \cap \Gamma^q =$.

Special attention requires electrical boundary conditions at crack surfaces. In this paper, it is assumed zero normal charge flux at crack surfaces following [Deeg (1980)] and [Pak (1992)],

$$D_n^+ = D_n^- = 0 \tag{13}$$

This assumption is based on other two: (i) there is no external charge at any of the crack surfaces, and (ii) the electrical induction of the void between both crack surfaces is zero.

3 BEM formulation

3.1 Traction boundary integral equation

Consider a piezoelectric body occupying the volume Ω bounded by a regular surface Γ. Neglecting body forces, the classical integral representation for an internal point $\mathbf{y} \in \Omega$ is stated as follows,

$$U_K(\mathbf{y}) + \int_\Gamma T^*_{KM}(\mathbf{x}-\mathbf{y}) U_M(\mathbf{x}) d\Gamma_x - \int_\Gamma U^*_{KM}(\mathbf{x}-\mathbf{y}) T_M(\mathbf{x}) d\Gamma_x = 0 \tag{14}$$

where U^*_{KM}, T^*_{KM} are the piezoelectric fundamental solution extended displacement and extended traction matrices respectively, which for the case of an elastically transversely isotropic behaviour, as considered in this paper, is found in [Dunn and Wienecke (1996)].

The integral representation for the traction components, is obtained by differentiation of Eq. 14 with respect to point $\mathbf{y}$ and combining according to Eq. 8,

$$T_J(\mathbf{y}) + \int_\Gamma s^*_{iMJ}(\mathbf{x}-\mathbf{y}) N_i(\mathbf{y}) U_M(\mathbf{x}) d\Gamma_x - \int_\Gamma d^*_{iMJ}(\mathbf{x}-\mathbf{y}) N_i(\mathbf{y}) T_M(\mathbf{x}) d\Gamma_x = 0 \tag{15}$$

where $N_i(\mathbf{y}) \overset{\text{def}}{=} n_i(\mathbf{y})$, and terms s^*_{iMJ}, d^*_{iMJ} are defined as,

$$s^*_{iMJ}(\mathbf{x}-\mathbf{y}) \overset{\text{def}}{=} \frac{\partial}{\partial y_l} T^*_{KM}(\mathbf{x}-\mathbf{y}) E_{iJKl} \tag{16}$$

$$d^*_{iMJ}(\mathbf{x}-\mathbf{y}) \overset{\text{def}}{=} \frac{\partial}{\partial y_l} U^*_{KM}(\mathbf{x}-\mathbf{y}) E_{iJKl} \tag{17}$$

d^*_{iMJ} and s^*_{iMJ} are linear combination of first and second derivatives, respectively, of the extended displacement fundamental solution matrix. They are widely discussed in the next section and reported in Appendix A.

It is necessary to take a limit to the boundary in order to get the integral representation for a smooth boundary point $\mathbf{y}$. The integrals in Eq. 15 are divided in two parts. One extends over a part of the boundary Γ_0 close to the collocation point, where the singularities will appear. The other extends over the rest of the boundary $\Gamma - \Gamma_0$.

At this point, a series expansion around the collocation point $\mathbf{y}$ is carried out,

$$U_K(\mathbf{x}) = U_k(\mathbf{y}) + U_{K,h}(\mathbf{y})(x_h - y_h) + O(r^{1+\alpha}) \tag{18}$$

$$T_K(\mathbf{x}) = \Sigma_{hK}(\mathbf{x}) n_h(\mathbf{x}) = \Sigma_{hK}(\mathbf{y}) n_h(\mathbf{x}) + O(r^\alpha) \tag{19}$$

which are substracted and added back from the extended displacement and tractions field in the

part of the integrals Γ_0 close to $\mathbf{y}$. After some analytical development and some simple algebra manipulation, the strong singularity and hipersingularity appeared in terms d^*_{iMJ} and s^*_{iMJ}, respectively, are regularized by means of Stokes' theorem. The process is presented in detail in [Dominguez, Ariza, and Gallego (2000)] for isotropic materials and [Ariza and Dominguez (2004)] for transversely isotropic materials. The extension to piezoelectricity requires some algebra but is completely analogous to the elasticity cases. The final expression for the traction boundary integral equation (BIE) is,

$$\begin{aligned}
&\frac{1}{2}T_J(\mathbf{y}) + \int_{\Gamma_0} \Big\{ s^*_{iMJ}(\mathbf{x}\text{-}\mathbf{y}) N_i(\mathbf{y}) \Big[U_M(\mathbf{x}) \\
&\quad - U_M(\mathbf{y}) - U_{M,h}(\mathbf{y})(x_h - y_h) \Big] \\
&\quad - d^*_{iMJ}(\mathbf{x}\text{-}\mathbf{y}) N_i(\mathbf{y}) \big[T_M(\mathbf{x}) - T_M(\mathbf{y}) \big] \Big\} d\Gamma_x \\
&\quad + \Big[U_M(\mathbf{y}) I_{MJ}(\mathbf{x}\text{-}\mathbf{y}) + U_{M,h}(\mathbf{y}) J_{MhJ}(\mathbf{x}\text{-}\mathbf{y}) \\
&\quad + T_M(\mathbf{y}) K_{MJ}(\mathbf{x}\text{-}\mathbf{y}) \Big] \\
&\quad + \int_{\Gamma - \Gamma_0} \Big\{ s^*_{iMJ}(\mathbf{x}-\mathbf{y}) N_i(\mathbf{y}) U_M(\mathbf{x}) \\
&\quad - d^*_{iMJ}(\mathbf{x}-\mathbf{y}) N_i(\mathbf{y}) T_M(\mathbf{x}) \Big\} d\Gamma_x = 0
\end{aligned} \tag{20}$$

where Γ_0 stands for the part of the boundary close to the collocation point $\mathbf{y}$, i.e., the elements containing the collocation point, being $\Gamma - \Gamma_0$ the rest of the boundary. The terms I_{MJ}, J_{MhJ} and K_{MJ} are the limit values at the surface of a sphere of radius $\varepsilon \to 0$ centered at $\mathbf{y} \in \Gamma$ of the result of application of Stokes' theorem to the regular part of the integral $\int_{\Gamma - e_\varepsilon} s^*_{iMJ} N_i d\Gamma_x$, $\int_{\Gamma - e_\varepsilon} s^*_{iMJ} N_i (x_h - y_h)\, d\Gamma_x$ and $\int_{\Gamma - e_\varepsilon} d^*_{iMJ} N_i d\Gamma_x$ respectively, with e_ε being the projection of the sphere over the boundary Γ and Γ_ε the outward half surface of the sphere. Eq. 20 is used for collocation points that belong to the crack surface. When this occurs, the free term in Eq. 20 becomes $T_J(y)$ for a self-equilibrated crack. The reader is referred to [Dominguez, Ariza, and Gallego (2000)] and [Ariza and Dominguez (2004)] for details. The terms I_{MJ}, J_{MhJ} and K_{MJ} contain only regular and weakly singular integrals. The regularisation process to get them is explained in the next section. Explicit expressions for terms I_{MJ}, J_{MhJ} and K_{MJ} can be found in [Solis (2007)].

3.2 Fundamental solution and kernel regularisation

The fundamental solution used in this paper is that for 3D transversely isotropic media presented in [Dunn and Wienecke (1996)]. This solution is obtained using a formulation where the three displacements and the electric potential are derived from two potential functions. The main advantage of this solution among others is the fact that it can be written as a close form expression. After differentiation of the extended displacements matrix, the extended tractions matrix is,

$$T^*_{KM}(\mathbf{x}-\mathbf{y}) = \frac{\partial}{\partial x_c} U^*_{BK}(\mathbf{x}-\mathbf{y})\, E_{aMBc} n_a(\mathbf{x}) \tag{21}$$

So, after inclusion of this equation into Eq. 16,

$$s^*_{iMJ}(\mathbf{x}-\mathbf{y}) = \frac{\partial}{\partial y_l} \frac{\partial}{\partial x_c} U^*_{BK}(\mathbf{x}-\mathbf{y})\, E_{iJKl} E_{aMBc} n_a(\mathbf{x}) \tag{22}$$

First and second derivatives of the extended displacement matrix to reach Eq. 17, Eq. 21 and Eq. 22 are given in Appendix A.

The terms s_{iMJ} and d_{iMJ} in Eq. 20 are hypersingular and singular of the order r^{-3}, r^{-2} when $r \to 0$, respectively. Under the assumption of plane crack, such that, $(\mathbf{x}-\mathbf{y}) \cdot \mathbf{n} = 0, \forall \{\mathbf{x}, \mathbf{y}\} \in \Gamma_{cr}$, with Γ_{cr} the crack surface and taking into consideration axis z as the material axis of symmetry and assuming that Γ_{cr} lies on $z = 0$, singularities in I_{MJ} and J_{MhJ} are shifted away by taking into account the following expressions and Stokes' theorem,

$$\frac{n_3 N_3 r_{,h}}{r^2} = \nabla \times \left[\frac{(\mathbf{e}_h \times \mathbf{N})}{r} \right] \cdot \mathbf{n} \tag{23}$$

for kernels in I_{MJ}, for those in J_{MhJ},

$$\frac{n_3 N_3 r_{,h} r_{,c} r_{,l}}{r^2} = \frac{1}{3}\delta_{cl}\nabla\times\left[\frac{(\mathbf{e}_h\times\mathbf{N})r_{,l}^2}{r}\right]\cdot\mathbf{n} + \frac{1}{3}\delta_{hl}\nabla\times\left[\frac{(\mathbf{e}_c\times\mathbf{N})r_{,l}^2}{r}\right]\cdot\mathbf{n} + \frac{1}{3}\delta_{ch}\nabla\times\left[\frac{(\mathbf{e}_l\times\mathbf{N})r_{,h}^2}{r}\right]\cdot\mathbf{n} + \frac{2}{3}\delta_{cl}\delta_{ch}\nabla\times\left[\frac{(\mathbf{e}_h\times\mathbf{N})}{r}\right]\cdot\mathbf{n} - \frac{2}{3}\delta_{cl}\delta_{ch}\nabla\times\left[\frac{(\mathbf{e}_h\times\mathbf{N})r_{,c}^2}{r}\right]\cdot\mathbf{n} \quad (24)$$

and for K_{MJ},

$$\frac{r_{,l}N_k - r_{,k}N_l}{r^2} = e_{lkj}\nabla\times\frac{1}{r}\mathbf{e}_j\mathbf{n} \quad (25)$$

e_{lkj} being the permutation symbol, $\mathbf{r}=\mathbf{x}-\mathbf{y}$, $r=|\mathbf{x}-\mathbf{y}|$, and $\mathbf{e}_h$ the canonical Cartesian vectors for $h=1,2,3$.

The order of the singularity is diminished performing a regularisation of the kernels appeared in I_{MJ} and J_{MhJ} by means of Stokes' theorem. Thus, for a plane crack, the terms I_{MJ}, J_{MhJ} and K_{MJ} transform into regular line integrals.

3.3 Computer implementation

At this point, some important computational issues and numerical treatment of Eq. 20 are discussed. Once the regularisation process has been developed for cases where the integration becomes singular or hypersingular, the formulation is greatly simplified under the assumption of plane crack, which addresses to regular line integration only.

For problems of cracks embedded in a piezoelectric solid domain, the traction BIE Eq. 20 is dealt in the sense of crack opening displacement and potential increment at both crack surfaces (COD) as basic unknowns to avoid the need of writing an equation at each crack surface. Obviously, at crack front, the crack opening displacement (COD) is equal to zero and consequently, it is not considered in the problem. Under crack boundary conditions (Eq. 13) and considering a self-equilibrated crack, $\Delta T_M(\mathbf{y})=0, \mathbf{y}\in\Gamma_{cr}$, the term K_{MJ} is cancelled out.

The analysis of cracks in an infinite solid only requires of the traction integral equation over one crack surface; COD being the only unknowns. In the case of cracks in a bounded domain, the collocation strategy is divided for points $\mathbf{y}\in\Gamma_{cr}$, where Eq. 20 is used as explained above, while for $\mathbf{y}\in\Gamma_{ex}=\Gamma-\Gamma_{cr}$ the classical BIE in terms of displacements is used. In the case of a border crack, such that the exterior and crack boundary $\Gamma_{cr}\cap\Gamma_{ex}\neq 0$, share some nodal points, since these collocation points are separately treated by classical and traction BIE, basic unknowns are displacements and electric potential. To do so, the classical BIE has to be written for crack nodal points in addition to traction BIE.

Discretization of Eq. 20 for collocation points on the crack surface, is easily implemented once two requierements are fulfilled: (1) the boundary extended displacement U_M satisfies the Holder continuity condition $U_M\in C^{1,\alpha}$ at $\mathbf{y}$; and (2) derivatives $\mathbf{y}$ of the extended displacements at collocation point exist in the boundary integral equation. Following [Gallego and Dominguez (1996)] for two dimensions and straightforward of [Ariza and Dominguez (2004)], these two requirements are automatically fulfilled if one discretizes the boundary using quadratic elements and collocates at points inside the element. Accurate results are obtained in [Ariza and Dominguez (2004)] for points with natural coordinates $\xi_{1,2}=\pm 0.75$. Elements with one side at the crack front are quarter-point elements with nine nodes on a plane and two straight line sides perpendicular to the crack front, see Figure 1. Displacement interpolation over these elements reproduce the profile of the extended displacements field as the square root of the distance to crack front [Ariza, Saez, and Dominguez (1997)].

3.4 ESIF evaluation

The piezoelectric problem, understood as an extension of the anisotropic theory of elasticity to piezoelectric materials, can be analyzed through

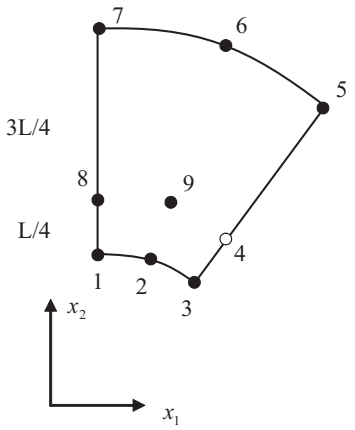

Figure 1: Nine node quarter-point quadratic element.

the Stroh's 2D formalism [Stroh (1962)]. In that case, the solution of the extended crack displacement problem to find is of the form,

$$U_K = A_K f(\mathbf{m}\cdot\mathbf{x} + p\mathbf{n}\cdot\mathbf{x}) \tag{26}$$

where $\mathbf{m}$ and $\mathbf{n}$ are two normal unit vectors in the plane perpendicular to the crack front.

It can be shown [Deeg (1980)], by substitution of Eq. 26 into Eq. 1, that a non-trivial solution for A_K exists, such that,

$$\left|(mm)_{JK} + p\left[(nm)_{JK} + (mn)_{JK}\right] + p^2(nn)_{JK}\right| = 0 \tag{27}$$

which can be posed as an eigenvalue problem $|\mathbf{N} - p_\alpha \mathbf{I}|$=0 where $\mathbf{N}$ is an 8×8 real matrix for 3D problems defined by,

$$\mathbf{N} = \begin{bmatrix} (nn)^{-1}(nm) & (nn)^{-1} \\ (mn)(nn)^{-1}(nm) - (mm) & (mn)(nn)^{-1} \end{bmatrix} \tag{28}$$

and $\mathbf{I}$ is the 8×8 unit matrix. For each eigenvalue p_α there is an eigenvector that can be written as,

$$\Xi_\alpha = \begin{Bmatrix} \mathbf{A}_\alpha \\ \mathbf{L}_\alpha \end{Bmatrix} \tag{29}$$

The above equation can be solved in terms of only the material constants, since the eigenvectors are independent of the base vectors $\mathbf{m}$ and $\mathbf{n}$ [Barnett and Lothe (1975)],

$$\left|C_{1JK1} + p\left[C_{1JK3} + C_{1KJ3}\right] + p^2 C_{3JK3}\right| = 0 \tag{30}$$

By identifying Eq. 27 and Eq. 30, one can obtain matrices $\mathbf{A}$ and $\mathbf{L}$ for each one of the four eigenvalues with positive imaginary part.

Finally, the electric -stress displacement intensity factor (ESIF) are,

$$\begin{Bmatrix} K_{II} \\ K_{III} \\ K_I \\ K_{IV} \end{Bmatrix} = \sqrt{\frac{\pi}{2L}}\, Re(\mathbf{Y})^{-1} \begin{Bmatrix} \Delta u_n \\ \Delta u_t \\ \Delta u_z \\ \Delta\Phi \end{Bmatrix} \tag{31}$$

with $\mathbf{Y} = \sqrt{-1}\mathbf{A}\mathbf{L}^{-1}$. COD of the above expression, are computed at quarter-point nodes, L being the length of the quarter-point element in the normal direction to the crack front. It is assumed that z is the material symmetry axis perpendicular to the crack plane, t-axis is tangent to the crack front line and n-axis is perpendicular to the other two.

4 Numerical examples

In order to validate the present technique, two problems of cracks in piezoelectric solids are studied next. The first example corresponds to a penny shaped crack in an infinite domain. This is probably the most simple 3D piezoelectric fracture mechanics problem. It can be easily analyzed with the present technique and is the only problem for which there exist a close form analytical solution. Its solution with the present approach requires only of the use of the traction BIE at nodal points on one of the crack surfaces. The second example, corresponds to a crack in a cylindrical body. This problem is studied using the mixed formulation; i.e., writing the tractions BIE for nodal points on one of the crack surfaces and the classical displacements BIE at nodes that belong to the body external surface. The material is assumed to be a PZT4 ceramic with the electromechanical properties listed in Table 1, for both examples.

Table 1: Material properties for piezoelectric material PZT-4 used in the numerical examples.

Elastic constants ($\times 10^{10} N/m^2$)	C_{11}	13.9
	C_{12}	7.78
	C_{13}	7.43
	C_{33}	11.3
	C_{44}	2.56
Piezoelectric constants (C/m^2)	e_{31}	-6.98
	e_{33}	13.84
	e_{15}	13.44
Dielectric constants ($\times 10^{-9} C/(V \cdot m)$)	ε_{11}	6.00
	ε_{33}	5.47

4.1 Penny shaped crack in infinite domain

This basic problem of 3D fracture mechanics has been extensively used as a benchmark problem for different types of materials and loading cases. In the case of piezoelectric materials, the problem has been studied analytically by several authors in the last ten years. [Huang (1997)] obtained a solution in terms of rather complicated expressions. The same year [Zhao, Shen, Liu, and Liu (1997a)] obtained a simple close form expressions for the displacement and electric potential discontinuities (COD) at the crack faces as well as for the electric-stress intensity factors (ESIF). [Chen, Shioya, and Ding (2000)] also obtained a close form expression for the ESIF. The K_I and K_{IV} ESIF for a crack under uniform internal pressure (or uniform traction at infinity), or under a uniform electric displacement at the crack faces (or at infinity) are,

$$K_I = 2\sqrt{\frac{a}{\pi}}\sigma_z \quad K_{IV} = 2\sqrt{\tfrac{a}{\pi}}D_z \tag{32}$$

respectively. In these expressions a is the crack radius, σ_z the internal pressure or traction at infinity and D_z is the electric displacement at crack faces or at infinity. It is worth to mention that both ESIF are uncoupled. K_I depends only on the mechanical load and K_{IV} only on the electric load. This fact does not mean either that the mechanical load does not produce a discontinuity of the electric potential at the crack surface, or that the electric load does not produce a displacement discontinuity at the crack surfaces.

In order to study this problem with the present technique, the crack surface is discretized into 64 nine-node quadratic elements as shown in Figure 2. The elements at the crack front are quarter-point elements. The traction BIE has to be written only for one of the crack faces.

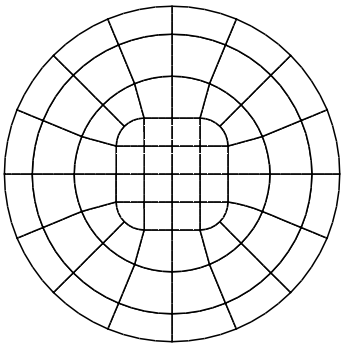

Figure 2: Penny-shaped crack discretization (64 elements)

Figure 3 shows the crack opening displacement in normal direction and the electric potential discontinuity along the radius when the crack is under internal pressure and under electric displacement. Results are compared in the figure with those given by [Zhao, Shen, Liu, and Liu (1997b)]. The agreement between both sets of results is very good. It can be seen from the figure that displacements due to the electric charge produce the same results that the electric displacement due to a mechanical load as expected. This fact shows the electro-mechanical coupling regardless the fact that this coupling does not affect the ESIF.

ESIF obtained from the extended displacements at quarter-point nodes according to Eq. 31 are given in Table 2. Relative error as compared to the analytical solution given by Eq. 32 are also shown. The accuracy of the computed K_I and K_{IV} ESIF is of the order of 0.5% in both cases.

Mode-II and mode-III ESIF for a penny shaped crack in an infinity piezoelectric solid under uniform shear traction have also been studied re-

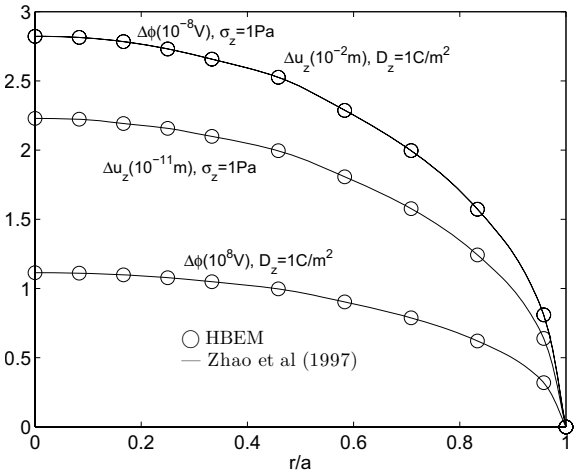

Figure 3: Radial profile of relative displacements and electric potential discontinuities. a(m) is the radius of the crack. σ_z (Pa) is the internal pressure or traction at infinity for mechanical load case. D_z (C/m^2) is the electric displacement at the crack faces or at infinity for electrical load case

Table 2: Computed ESIFs for penny shaped crack and relative error

	HBEM	Error
$K_I/p/\sqrt{a/\pi}$	1.9895	0.525%
$K_{IV}/D_z/\sqrt{a/\pi}$	1.9901	0.495%

cently. [Kogan, Hui, and Molkov (1995)] studied the problem as a degenerated of an spheroidal inclusion. They obtained a solution for the ESIF in terms of a system of equations and did not present numerical values. [Chen, Shioya, and Ding (2000)] obtained rather complicated expressions for ESIF. [Zhao, Shen, Liu, and Liu (1997a)] presented compact expressions for ESIF K_{II} and K_{III} for the problem at hand. Figure 4 shows the dimensionless K_{II} and K_{III} ESIF along the crack front computed with the present approach using the BE mesh shown in Figure 2. The computed results are compared in the figure with those obtained by [Zhao, Shen, Liu, and Liu (1997a)]. Both sets of results show a very good agreement. Because of the symmetry, results for one quarter of the crack are shown.

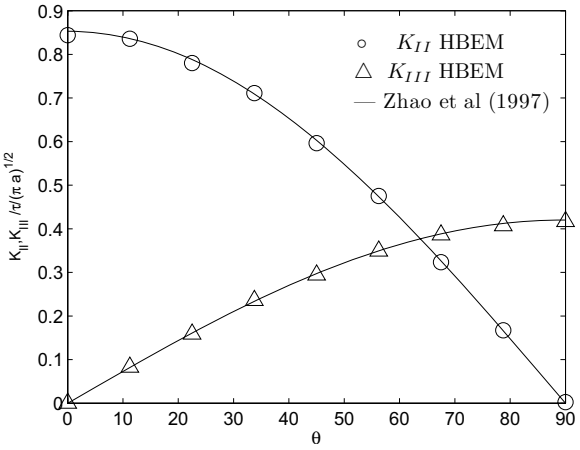

Figure 4: Mode II and mode III results for penny-shaped crak

4.2 Penny shaped crack in cylindrical bar

A penny shaped crack embedded in a cylindrical bar is studied next. The specimen is under uniform traction $\sigma_z = 1Pa$ or under uniform electric displacement $D_z = 1C/m^2$ at the two opposite exterior faces, while the rest of the boundary is free of electric displacement and traction. The discretization of the external boundary of the body is shown in Figure 5, the crack discretization being the same as in the previous example. For collocation points $\mathbf{y}$ on the exterior boundary the classical displacement BIE is implemented, while for $\mathbf{y}$ on the crack surface the traction BIE is used.

In order to validate the propose BEM formulation, the same geometry and properties given in [Sanz, Ariza, and Dominguez (2005)] are considered. Those authors studied the problem using the classical displacement BIE formulation and a subdomain technique. The geometrical relations are $H = R = 2a$, (see Figure 5). The piezoelectric material is considered to be PZT4 with material constants as given in table 1. Crack surface displacement and electric potential values for this problem can be seen in Figure 6.

Computed values of the ESIF are reported in table 3 and compared with those obtained by [Sanz, Ariza, and Dominguez (2005)], both for mechanical and electric loading. They are normalized with respect the applied traction σ_z and the electric displacement D_z^* (C/m^2) having the same numerical

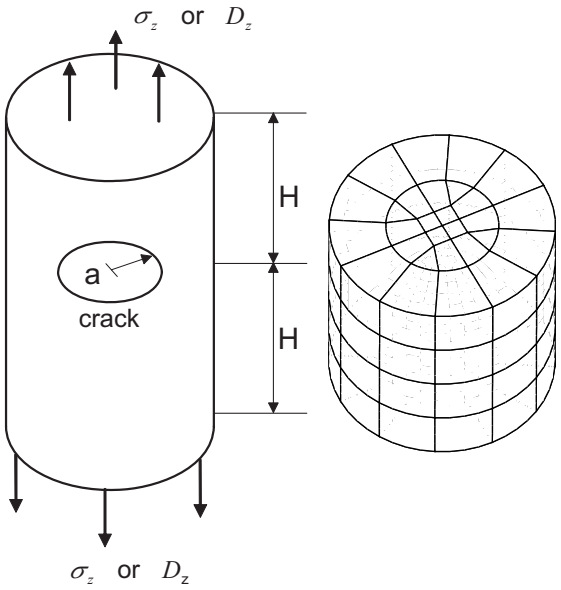

Figure 5: Penny shaped crack embbedded in cylindrical bar subjected to uniform traction or electric displacement. Below BEM mesh.

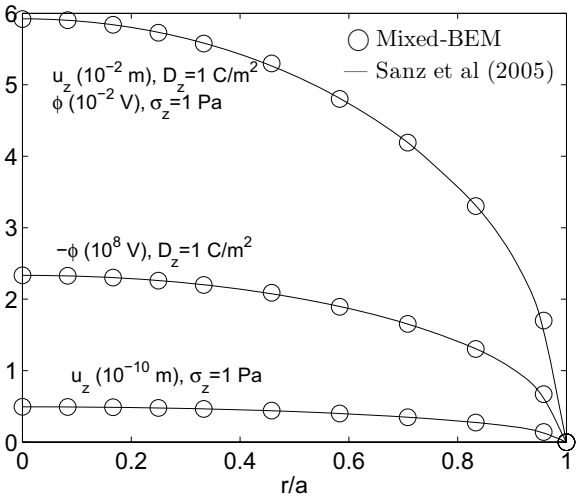

Figure 6: Crack surface displacement and electric potential for penny shaped crack embbeded in cylindrical bar, obtained by classical formulation [Sanz, Ariza, and Dominguez (2005)] and mixed formulation (present work).

value as σ_z (GPa) in the first case, and with respect to the applied electric displacement D_z and the traction σ_z^* (GPa) having the same numerical value as D_z (C/m^2), in the second case. Results obtained with the present mixed BE technique and those obtained using the classical displacement BIE are in quite good agreement. To the authors knowledge, no more results for this problem exist in the literature.

Table 3: Normalized ESIF for both mechanical and electric loading.

Mech. load	$K_I/(\sigma_z\sqrt{\pi a})$	$K_{IV}/(D_z^*\sqrt{\pi a})$
Classic. form	0.691	0.0075
Present work	0.691	0.0068
Elect. load	$K_I/(\sigma_z^*\sqrt{\pi a})$	$K_{IV}/(D_z\sqrt{\pi a})$
Classic. form	$1.81\cdot10^{-4}$	0.663
Present work	$1.92\cdot10^{-4}$	0.664

5 Conclusions

A general mixed boundary element formulation for three-dimensional piezoelectric fracture mechanics problems has been presented. The main difficulty in the development of the approach is the differentiation of the fundamental solution to obtain the extended traction integral equation kernels and their transformation in a way such that integrals can be regularized by simple analytical transformation. This has allowed for derivation and implementation of a simple approach suitable for crack problems in solids of any geometry and under general mechanical and electrical boundary conditions.

The approach has been applied to two different crack problems. In the first one, the crack is in a boundless domain, and in the second in a finite solid. Mechanical and electrical loads have been applied. Extended crack opening displacements and electric and stress intensity factors have been evaluated in a simple way. The present results are in very good agreement with solutions obtained by other authors. Since the approach is general and simple to use, the authors will analyze and present results for crack problems with different geometries, material properties and loading conditions in a forthcoming paper.

Acknowledgement: This work has been supported by the Ministerio de Educación y Ciencia

of Spain. (Project: DPI2004-08147-C02-02). The financial support is gratefully acknowledged.

References

Ariza, M. P.; Dominguez, J. (2004): . Boundary element formulation for 3D transversely isotropic cracked bodies. *Int. J. Numer. Meth. Eng.*, vol. 60, pp. 719–753.

Ariza, M. P.; Saez, A.; Dominguez, J. (1997): . A singular element for three dimensional fracture mechanics analysis. *Eng. Anal. Bound. Elem.*, vol. 20, pp. 275–285.

Barnett, D. M.; Lothe, J. (1975): . Dislocations and line charges in anisotropic piezoelectric insulators. *Physica Status Solidi (b)*, vol. 67, pp. 105–111.

Chen, M. (2003): . Application of finite-part integrals to the three dimensional fracture problems for piezoelectric media. Part I: hypersingular equation and theoretical anlysis. *Int. J. Fract.*, vol. 121, pp. 133–148.

Chen, M. (2003): . Application of finite-part integrals to the three dimensional fracture problems for piezoelectric media. Part II: numerical analysis. *Int. J. Fract.*, vol. 121, pp. 149–161.

Chen, M. (2005): . 3D mode I crack analysis of piezoelectrics. *Comput. Methods Appl. Mech. Engrg.*, vol. 194, pp. 957–968.

Chen, T.; Lin, F. (1995): . Boundary integral formulations for three-dimesional anisotropic piezoelectric bodies. *Comput. Mech.*, vol. 15, pp. 485–496.

Chen, W.; Shioya, T.; Ding, H. (2000): . A penny shaped crack in piezoelectrics: resolved. *Int. J. Fracture*, vol. 105, pp. 49–56.

Deeg, W. F. (1980): . *The analysis of dislocation, crack and inclusion problems in piezoelectric solids*. PhD Thesis, Stanford University.

Ding, H.; Chen, W.; ; Jiang, A. (2004): . Green's functions and boundary element method for transversely isotropic piezoelectric materials. *Eng. Anal. Bound. Elem.*, vol. 28, pp. 975–987.

Ding, H.; Liang, J. (1999): . The fundamental solution for transversely isotropic piezoelectricity and boundary element method. *Comput. Struct.*, vol. 71, pp. 447–455.

Dominguez, J.; Ariza, M. P.; Gallego, R. (2000): . Flux and traction boundary elements without hypersingular or strongly singular integrals. *Int. J. Numer. Meth. Eng.*, vol. 48, pp. 111–135.

Dunn, M. L.; Wienecke, H. A. (1996): . Green's function for transversely isotropic piezoelectric solids. *Int. J. Solids and Str.*, vol. 33, pp. 4571–4581.

Gallego, R.; Dominguez, J. (1996): . Hypersingular BEM for transient elastodynamics. *Int. J. Numer. Meth. Eng.*, vol. 39, pp. 601–611.

Garcia-Sanchez, F.; Saez, A.; Dominguez, J. (2005): . Anisotropic and Piezoelectric Materials Fracture Analysis by BEM. *CMES: Computer Modeling in Engineering and Sciences*, vol. 83, pp. 804–820.

Gross, D.; Rangelov, T.; Dineva, P. (2005): . 2D wave scattering by a crack in a piezoelectric plane using traction BIEM. *Str. Int. Dur.*, vol. 1, pp. 35–48.

Huang, J. H. (1997): . A fracture criterion of a penny-shaped crack in transversely isotropic piezoelectric media. *Int. J. Solids Str.*, vol. 34, pp. 2631–2644.

Kogan, L.; Hui, C. Y.; Molkov, V. (1995): . Stress and induciton field of a spheroidal inclusion or a penny-shaped crack in a transversely isotropic piezoelectric material. *Int. J. Solids Str.*, vol. 33, pp. 2719–2737.

Kuna, M. (1998): . Finite element analyses of crack problems in piezoelectric structures. *Comput. Mat. Science*, vol. 13, pp. 67–80.

Lin, S.; Narita, F.; Shindo, Y. (2003): . Electroelastic analysis of a penny-shaped crack in a piezoelectric ceramic under mode I loading. *Mechanics Researh communications*, vol. 30, pp. 371–386.

Pak, Y. E. (1990): . Crack extension force in a piezoelectric material. *J. Appl. Mech.*, vol. 57, pp. 647–653.

Pak, Y. E. (1992): . Linear electro-elastic fracture mechanics of piezoelectric materials. *Int. J. Fract.*, vol. 54, pp. 79–100.

Pan, E. (1999): . A BEM analysis of fracture mechanics in 2D anisotropic piezoelectric solids. *Eng. Anal. Bound. Elem.*, vol. 23, pp. 67–76.

Parton, V. (1976): . Fracture Mechanics of Piezoelectric Materials. *Acta Astronautica*, vol. 3, pp. 671–683.

Saez, A.; Garcia-Sanchez, F.; Dominguez, J. (2006): . Hypersingular BEM for dynamic fracture in 2-D piezoelectric solids. *Comput. Methods Appl. Mech. Engrg.*, vol. 196, pp. 235–246.

Sanz, J. A.; Ariza, M. P.; Dominguez, J. (2005): . Three-dimensional BEM for piezolectric fracture analysis. *Eng. Anal. Bound. Elem.*, vol. 29, pp. 586–596.

Sellountos, E. J.; Vavourakis, V.; Polyzos, D. (2005): . A new singular/hypersingular MLPG (LBIE) method for 2D elastostatics. *CMES: Computer Modeling in Engineering and Sciences*, vol. 7, pp. 35–48.

Shang, F.; Kuna, M.; Abendroth, M. (2003): . Finite element analyses of three-dimensional crack problems in piezoelectric structures. *Engrg. Fract. Mech.*, vol. 70, pp. 143–160.

Sladek, J.; Sladek, V.; Zhang, C.; Garcia-Sanchez, F.; Wunsche, M. W. (2006): . Meshless local Petrov-Galerkin method for plane piezoelectricity. *CMC: Computers, Materials & Continua*, vol. 4, pp. 109–118.

Solis, M. (2007): . *Numerical model for three-dimensional transversely isotropic and piezoelectric cracked solids*. PhD Thesis (in Spanish), University of Sevilla.

Sosa, H. (1992): . On fracture mechanics of piezoelectric solids. *Int. J. Solids Struc.*, vol. 29, pp. 2613–2622.

Stroh, A. N. (1962): . Steady state problems in anisotropic elasticity. *J. Mat. Phys.*, vol. 41, pp. 77–103.

Suo, Z.; Kuo, C.-M.; Barnett, D.; Willis, J. (1992): . Fracture mechanics for piezoelectric ceramics. *Journal of Mech. Phys. Solids*, vol. 40, pp. 739–765.

Zhao, M.; Shen, Y.; Liu, Y.; Liu, G. (1997): . Isolated crack in three-dimensional piezoelectric solid:Part I-solution by Jankel transform. *Theor. Appl. Fract. Mech.*, vol. 21, pp. 129–139.

Zhao, M.; Shen, Y.; Liu, Y.; Liu, G. (1997): . Isolated crack in three-dimensional piezoelectric solid:Part II-stress intensity factors for circular crack. *Theor. Appl. Fract. Mech.*, vol. 21, pp. 141–149.

Appendix A: First and second derivatives of the fundamental solution

First and second derivatives of the fundamental solution extended displacement matrix Dunn and Wienecke (1996), are necessary in order to evaluate expressions in Eq. 17, Eq. 21 and Eq. 22, both with respect to collocation point **y** and integration **x** point.

First derivatives of fundamental extended displacement, for $x_3 - y_3 \geq 0$, with respect to the integration point x are stated as follows,

$$\frac{\partial}{\partial x_m} U_{11} = D_0 \left[-\frac{r^*_{0,m}}{r^{*2}_0} + z_2^2 H_{0,m} - \frac{2z_2}{r_0 r^{*2}_0} \delta_{2m} \right] - \sum_{i=1}^{3} D_i \lambda_{i1} \left[-\frac{r^*_{i,m}}{r^{*2}_i} + z_1^2 H_{i,m} - \frac{2z_1}{r_i r^{*2}_i} \delta_{1m} \right] \quad (33)$$

$$\frac{\partial}{\partial x_m} U_{22} = D_0 \left[-\frac{r^*_{0,m}}{r^{*2}_0} + z_1^2 H_{0,m} - \frac{2z_1}{r_0 r^{*2}_0} \delta_{1m} \right] - \sum_{i=1}^{3} D_i \lambda_{i1} \left[-\frac{r^*_{i,m}}{r^{*2}_i} + z_2^2 H_{i,m} - \frac{2z_2}{r_i R^{*2}_i} \delta_{2m} \right] \quad (34)$$

$$\frac{\partial}{\partial x_m}U_{12} = D_0\left[\frac{z_2}{r_0 r_0^{*2}}\delta_{1m} - z_1 z_2 H_{0,m} + \frac{z_1}{r_0 r_0^{*2}}\delta_{2m}\right] + \sum_{i=1}^{3} D_i \lambda_{i2}\left[\frac{z_2}{r_i r_i^{*2}}\delta_{1m} - z_1 z_2 H_{i,m} + \frac{z_1}{r_i r_i^{*2}}\delta_{2m}\right] \tag{35}$$

$$\frac{\partial}{\partial x_m}U_{I=3:4,J=1:2} = \sum_{i=1}^{3} A_{iI}\lambda_{iJ}\left[\frac{\delta_{Jm}}{r_i r_i^*} - z_J\frac{r_{i,m}r_i^* + r_{i,m}^* r_i}{\left(r_i r_i^*\right)^2}\right] \tag{36}$$

$$\frac{\partial}{\partial x_m}U_{I=3:4,J=3:4} = -\sum_{i=1}^{3} A_{iI}\lambda_{iJ}\frac{r_{i,m}}{r_i^2} \tag{37}$$

with δ_{ij} the Kronecker's delta and $z_i \overset{\text{def}}{=} x_i - y_i$. Moreover, $r_i \overset{\text{def}}{=} \sqrt{z_1^2 + z_2^2 + \nu_i z_3^2}$, $r_i^* \overset{\text{def}}{=} r_i + \nu_i z_3$ for $i = 0:3$. The rest of terms are as follows,

$$r_{i,m} = \frac{\partial r_i}{\partial x_m} = \frac{z_m}{r_i}\left[1 + \left(\nu_i^2 - 1\right)\delta_{3m}\right] \quad \text{for } i = 0:3 \tag{38}$$

$$r_{i,m}^* = r_{i,m} + \nu_i \delta_{3m} \quad \text{for } i = 0:3 \tag{39}$$

$$H_{i,m} \overset{\text{def}}{=} -\frac{\partial}{\partial x_m}\left(\frac{1}{r_i r_i^{*2}}\right) = \frac{r_{i,m}r_i^{*2} + 2r_i r_i^* r_{i,m}^*}{\left(r_i r_i^{*2}\right)^2} \quad \text{for } i = 0:3 \tag{40}$$

where repeated indices does not mean summation.

The remaining terms of the first derivative of the fundamental extended displacement matrix solution, is found attending to the symmetry condition $\frac{\partial}{\partial x_m}U_{IJ} = \frac{\partial}{\partial x_m}U_{JI}$.

Since first derivative functions above are given for $z_3 = x_3 - y_3 \geq 0$, the opposite case, is automatically evaluated because of the symmetry, anti-symmetry conditions of these functions with respect to z_3. So, these functions fullfil $f(z_1,z_2,z_3) = -f(z_1,z_2,-z_3)$ for $(I,J,m) = (3:4,1:2,1:2)$ and $(I,J,m) = (1,1,3),(2,2,3),(2,1,3),(3,3,3),(3,4,3),(4,4,3)$. Moreover, $f(z_1,z_2,z_3) = f(z_1,z_2,-z_3)$ for the rest of cases.

When the first derivative of the fundamental solution extended displacement matrix with respect to the collocation point **y** is needed, Eq. 17, the following relation is used, $\frac{\partial}{\partial x_m}U_{IJ} = -\frac{\partial}{\partial y_m}U_{IJ}$.

Above expressions are given in terms of constants $A_{iI}, \lambda_{iJ}, D_i, D_0, \nu_i$ and ν_0, which only depend on the material properties. Coefficients $-1/\nu_1^2$,$-1/\nu_2^2$ and $-1/\nu_3^2$ are defined as the three roots of the following polynomial,

$$s^3 + \frac{a}{d}s^2 + \frac{b}{d}s + \frac{c}{d} = 0 \tag{41}$$

where these three roots are either real or one real and the other two complex conjugates. The coefficients a, b, c and d are defined as,

$$\begin{aligned} a =& C_{11}\left(\varepsilon_{11}C_{33} + 2e_{15}e_{33}\right) - \varepsilon_{11}C_{13}\left(C_{13} + 2C_{44}\right) \\ &+ C_{44}\left(\varepsilon_{33}C_{11} + e_{31}^2\right) \\ &- 2e_{15}C_{13}\left(e_{31} + e_{15}\right) \end{aligned} \tag{42}$$

$$\begin{aligned} b =& C_{33}\left[\varepsilon_{11}C_{44} + \varepsilon_{33}C_{11} + e_{31}\left(e_{31} + e_{15}\right)\right] \\ &- C_{13}\varepsilon_{33}\left(C_{13} + 2C_{44}\right) \\ &+ \left(e_{31} + e_{15}\right)\left(C_{33}e_{15} - 2C_{13}e_{33}\right) \\ &+ e_{33}\left(C_{11}e_{33} - 2C_{44}e_{31}\right) \end{aligned} \tag{43}$$

$$c = C_{44}\left(\varepsilon_{33}C_{33} + e_{33}^2\right) \tag{44}$$

$$d = C_{11}\left(\varepsilon_{11}C_{44} + e_{15}^2\right) \tag{45}$$

The rest of constants present in the fundamental solution and its derivatives are defined as,

$$\lambda_{i1} = \left[\left(C_{13}+C_{44}\right)e_{33} - C_{33}\left(e_{31}+e_{15}\right)\right]\nu_i^3 + \left(C_{44}e_{31} - C_{13}e_{15}\right)\nu_i \quad (46)$$

$$\lambda_{i2} = \lambda_{i1} \quad (47)$$

$$\lambda_{i3} = -C_{44}e_{33}\nu_i^4 - e_{15}C_{11} - \left[e_{31}\left(C_{13}+C_{44}\right) - e_{33}C_{11} + e_{15}C_{13}\right]\nu_i^2 \quad (48)$$

$$\lambda_{i4} = C_{44}C_{33}\nu_i^4 + C_{44}C_{11} + \left[C_{13}\left(C_{13}+2C_{44}\right) - C_{11}C_{33}\right]\nu_i^2 \quad (49)$$

$$A_{13} = \left(\nu_1^2-1\right)\left[n_2^e\lambda_{31}\left(\nu_3^2-1\right) - n_3^e\lambda_{21}\left(\nu_2^2-1\right)\right] \cdot \frac{1}{2\pi\gamma_a} \quad (50)$$

$$A_{14} = \frac{\left(\nu_1^2-1\right)\left(\nu_2^2-1\right)\left(\nu_3^2-1\right)}{\nu_1\left(\nu_1^2-\nu_2^2\right)\left(\nu_1^2-\nu_3^2\right)}\frac{(-1)}{4\pi\gamma_e} \quad (51)$$

$$\nu_0 = \sqrt{\frac{C_{66}}{C_{44}}} \quad (52)$$

$$D_0 = \frac{1}{4\pi C_{44}\nu_0} \quad (53)$$

$$D_1 = \frac{\lambda_{24}\lambda_{33} - \lambda_{34}\lambda_{23}}{4\pi C_{44}\gamma_t} \quad (54)$$

being,

$$n_i^a = 2\Big[\lambda_{i1}\left(C_{13}+C_{44}\nu_i^2\right) + \nu_i\lambda_{i3}\left(C_{44}-C_{33}\right) + \nu_i\lambda_{i4}\left(e_{15}-e_{33}\right)\Big] \quad (55)$$

$$n_i^e = 2\Big[-\lambda_{i1}\left(e_{15}\nu_i^2+e_{31}\right) + \nu_i\lambda_{i3}\left(e_{33}-e_{15}\right) + \nu_i\lambda_{i4}\left(\varepsilon_{11}-\varepsilon_{33}\right)\Big] \quad (56)$$

$$\gamma_a = \left(\nu_1^2-1\right)\lambda_{11}\left(n_2^a n_3^e - n_3^a n_2^e\right) + \left(\nu_2^2-1\right)\lambda_{21}\left(n_3^a n_1^e - n_1^a n_3^e\right) + \left(\nu_3^2-1\right)\lambda_{31}\left(n_1^a n_2^e - n_2^a n_1^e\right) \quad (57)$$

$$\gamma_e = \left(\varepsilon_{11}-\varepsilon_{33}\right) \cdot \left[C_{11}\left(C_{44}-C_{33}\right) + C_{44}\left(C_{33}+2C_{13}\right) + C_{13}^2\right] + C_{11}\left(e_{33}-e_{15}\right)^2 + C_{33}\left(e_{31}+e_{15}\right)^2 - C_{44}\left(e_{33}+e_{31}\right)^2 + 2C_{13}\left[e_{15}\left(e_{15}+e_{31}-e_{33}\right) - e_{33}e_{31}\right] \quad (58)$$

$$\gamma_t = \nu_1\lambda_{11}\left(\lambda_{34}\lambda_{23} - \lambda_{24}\lambda_{33}\right) + \nu_2\lambda_{21}\left(\lambda_{14}\lambda_{33} - \lambda_{34}\lambda_{13}\right) + \nu_3\lambda_{31}\left(\lambda_{24}\lambda_{13} - \lambda_{14}\lambda_{23}\right) \quad (59)$$

Other terms A_{i3}, A_{i4} are given by permuting index i through A_{13}, A_{14} respectively. The same for D_i through D_1.

The second derivative of the fundamental solution extended displacement matrix with respect to the collocation and integration point, which appears in Eq. 22, yields to,

$$\frac{\partial}{\partial y_l}\frac{\partial}{\partial x_m}U_{11}^* = D_0\left[\frac{r_{0,ml}^* r_0^* - 2r_{0,l}^* r_{0,m}^*}{r_0^{*3}} - 2z_2\delta_{l2}H_{0,m} - z_2^2 H_{0,ml} + \delta_{2m}\left(\frac{2\delta_{2l}}{r_0 r_0^{*2}} - 2z_2 H_{0,l}\right)\right] + \sum_{i=1}^{3} D_i\lambda_{i1}\left[-\frac{r_{i,ml}^* r_i^* - 2r_{i,l}^* r_{i,m}^*}{r_i^{*3}} + 2z_1\delta_{l1}H_{i,m} + z_1^2 H_{i,ml} - \delta_{1m}\left(\frac{2\delta_{1l}}{r_i r_i^{*2}} - 2z_1 H_{i,l}\right)\right] \quad (60)$$

$$\frac{\partial}{\partial y_l}\frac{\partial}{\partial x_m}U^*_{22} = D_0\left[\frac{r^*_{0,ml}r^*_0 - 2r^*_{0,l}r^*_{0,m}}{r^{*3}_0} - 2z_1\delta_{l1}H_{0,m} - z_1^2H_{0,ml} + \delta_{1m}\left(\frac{2\delta_{1l}}{r_0r^{*2}_0} - 2z_1H_{0,l}\right)\right] + \sum_{i=1}^{3}D_i\lambda_{i1}\left[-\frac{r^*_{i,ml}r^*_i - 2r^*_{i,l}r^*_{i,m}}{r^{*3}_i} + 2z_2\delta_{l2}H_{i,m} + z_2^2H_{i,ml} - \delta_{2m}\left(\frac{2\delta_{2l}}{r_ir^{*2}_i} - 2z_2H_{i,l}\right)\right] \tag{61}$$

$$\frac{\partial}{\partial y_l}\frac{\partial}{\partial x_m}U^*_{I=3:4,J=1:2} = \sum_{i=1}^{3}A_{iI}\lambda_{iJ}\left[\delta_{Jl}\frac{r_{i,m}r^*_i + r_ir^*_{i,m}}{(r_ir^*_i)^2} + z_J\xi_{i,ml} + \delta_{Jm}\frac{r_{i,l}r^*_i + r_ir^*_{i,l}}{(r_ir^*_i)^2}\right] \tag{62}$$

$$\frac{\partial}{\partial y_l}\frac{\partial}{\partial x_m}U^*_{I=3:4,J=3:4} = \sum_{i=1}^{3}A_{iI}\lambda_{iJ}\frac{r_{i,ml}r_i - 2r_{i,l}r_{i,m}}{r^3_i} \tag{63}$$

$$\frac{\partial}{\partial y_l}\frac{\partial}{\partial x_m}U^*_{12} = D_0\left[-\frac{\delta_{1m}\delta_{2l}}{r_0r^{*2}_0} + z_2\delta_{1m}H_{0,l} - \frac{\delta_{2m}\delta_{1l}}{r_0r^{*2}_0} + z_1\delta_{2m}H_{0,l} + z_2z_1H_{0,ml} + \delta_{1l}z_2H_{0,m} + \delta_{2l}z_1H_{0,m}\right] + \sum_{i=1}^{3}D_i\lambda_{i2}\left[-\frac{\delta_{1m}\delta_{2l}}{r_ir^{*2}_i} + z_2\delta_{1m}H_{i,l} - \frac{\delta_{2m}\delta_{1l}}{r_ir^{*2}_i} + z_1\delta_{2m}H_{i,l} + z_2z_1H_{i,ml} + \delta_{1l}z_2H_{i,m} + \delta_{2l}z_1H_{i,m}\right] \tag{64}$$

where,

$$r^*_{i,ml} = \frac{\partial}{\partial x_m}\frac{\partial}{\partial x_l}r^*_i = \left[1 + (\nu_i^2 - 1)\delta_{3m}\right]\frac{\delta_{ml}r_i - z_mr_{i,l}}{r^2_{i,l}} = r_{i,ml} \tag{65}$$

$$H_{i,ml} = \frac{\partial}{\partial x_l}H_{i,m} = \Big[r_{i,ml}r^{*2}_i + 2r_{i,m}r^*_ir^*_{i,l} + 2(r_{i,l}r^*_ir^*_{i,m} + r_ir^*_{i,l}r^*_{i,m} + r_ir^*_ir^*_{i,ml})\Big](r_ir^{*2}_i) - 2(r_{i,m}r^*_i + 2r_ir^*_ir^*_{i,m}) \cdot (r_{i,l}r^{*2}_i + 2r_ir^*_ir^*_{i,l})/(r_ir^{*2}_i)^3 \tag{66}$$

$$\xi_{i,ml} \overset{\text{def}}{=} \frac{\partial}{\partial x_l}\left[\frac{r_{i,m}r^*_i + r^*_{i,m}r_i}{(r_ir^*_i)^2}\right] = \Big[(r_{i,ml}r^*_i + r_{i,m}r^*_{i,l} + r_{i,l}r^*_{i,m} + r_ir^*_{i,ml})(r_ir^*_i) - 2(r_{i,m}r^*_i + r_ir^*_{i,m})(r_{i,l}r^*_i + r_ir^*_{i,l})\Big]/(r_ir^*_i)^3 \tag{67}$$

Again, repeated indices does not mean summation. As for the case of the first derivative, expressions above are defined for $z_3 = x_3 - y_3 \geq 0$. The opposite case, is evaluated by means of symmetry and anti-symmetry relations with respect to z_3. Thus, $f(z_1,z_2,z_3) = -f(z_1,z_2,-z_3)$ for $(I,J,m,l) = (1:2,1:2,1:2,3),(3:4,3:4,1:2,3)$ taking into consideration $(I,J,m,l) = (J,I,m,l) = (J,I,l,m)$ and $f(z_1,z_2,z_3) = f(z_1,z_2,-z_3)$ for the rest of cases.